


Cite this: *RSC Adv.*, 2022, 12, 21932

# High efficiency and low operating voltage yellow phosphorescent organic light-emitting diodes with a simple doping-free structure

Jie Hua,<sup>a,b</sup> Jiaxin Li,<sup>ab</sup> Zhuolin Zhan,<sup>b</sup> Yuan Chai,<sup>ab</sup> Zeyuan Cheng,<sup>b</sup> Peiding Li,<sup>b</sup> He Dong<sup>ab</sup> and Jin Wang<sup>ab</sup>

Yellow phosphorescent organic light-emitting diodes (PhOLEDs) with high efficiency and a low operating voltage were reported through using a simple doping-free structure. The structure of the PhOLEDs was ITO/C<sub>60</sub>/MoO<sub>3</sub>/mCP/PO-01-TB/PO-T2T/Liq/Al. The np-type C<sub>60</sub>/MoO<sub>3</sub> heterojunction acted as hole injection layer, and the ultrathin PO-01-TB layer (0.1 nm) was inserted at the interface between mCP and PO-T2T to serve as yellow phosphorescent emitter. Detailed investigation suggested that the complete energy transfer occurred from the mCP/PO-T2T interfacial exciplex to yellow PO-01-TB. Furthermore, the np-type C<sub>60</sub>/MoO<sub>3</sub> heterojunction could supply more free charge carriers, giving rise to further enhanced PhOLED efficiency. By adjusting the thickness of the C<sub>60</sub>/MoO<sub>3</sub> heterojunction, a yellow PhOLED with a power efficiency of 71.6 lm W<sup>-1</sup> was demonstrated with an extremely low operating voltage of 3.79 V at 1000 cd m<sup>-2</sup>.

Received 11th June 2022

Accepted 22nd July 2022

DOI: 10.1039/d2ra03617g

rsc.li/rsc-advances

## 1. Introduction

Much endeavor has been made to pursue high performance organic light-emitting diodes (OLEDs) in the past three decades because of their huge potential applications in solid state lighting and full color flat panel displays.<sup>1–4</sup> According to the different types of emitting materials used in devices, OLEDs are divided into fluorescent OLEDs (FLOLEDs) and phosphorescent OLEDs (PhOLEDs). As compared with traditional fluorescent emitters, phosphorescent emitters can harvest both singlet S<sub>1</sub> and triplet T<sub>1</sub> excitons for electroluminescence (EL) owing to the heavy-atom effect, so that they can realize 100% internal quantum efficiency (IQE), showing a great potential for developing high-performance OLEDs.<sup>5–8</sup> To avoid the concentration quenching effects between phosphorescent molecules induced by strong intermolecular interaction, a host-guest doping system is normally adopted in PhOLEDs. This means that choosing a proper host for a phosphorescent emitter is a key strategy to achieve high efficiency PhOLEDs.

Traditional PhOLEDs usually use hole transport materials as host matrix. Unfortunately, this type host can render unbalance charge transport,<sup>9</sup> thus worsening the exciton quenching effects.<sup>8,10</sup> To address those issues, PhOLEDs utilizing neutral exciplex as co-host have attracted more attentions recently. The exciplex is formed through the charge transfer between electron transporting material (electron

donor) and hole transporting material (electron acceptor), showing obvious bipolar charge transport as well as high triplet energy, which reducing the polaron accumulation to restrain exciton quenching. Moreover, owing to small orbital overlap between the excited state and the ground state, most exciplex possess a small ΔE<sub>st</sub> (S<sub>1</sub>–T<sub>1</sub> energy splitting), which promotes the energy transfer process changing from Dexter energy transfer to Förster energy transfer in host-guest doping system.<sup>8,11–17</sup> For example, Park *et al.*<sup>16</sup> doped bis(2-phenylpyridine)(acetylacetonato) iridium(III) (Ir(ppy)<sub>2</sub>acac) into the exciplex co-host formed by 4,4',4''-tri(*N*-carbazolyl) triphenylamine(TCTA) and bis-4,6-(3,5-di-3-pyridylphenyl)-2-methylpyrimidine (B3PYMPM) to achieve green PhOLED with low turn-on voltage of 2.4 V and high external quantum efficiency (EQE) of 29.1% as well as low roll-off. Wang *et al.*<sup>17</sup> employed interfacial exciplex of (*N,N'*-di(naphth-1-yl)-*N,N'*-diphenyl-benzidine (NPB)/1,3,5 tris[*N*-(phenyl) benzimidazole]-benzene (TPBi) as co-host to fabricate a red PhOLED showing a high EQE of 17.2% and a low turn-on voltage of 2.6 V simultaneously. These results suggest that the exciplex with unique photophysical properties become a potential alternative for developing high performance PhOLEDs.

For the PhOLEDs, the efficient charge injection is another key factor for achieving high performance. For hole injection, P-type transition metal oxides-molybdenum trioxide (MoO<sub>3</sub>) with high transparency and work function shows strong hole injection ability, and has been widely used as hole injection layer (HIL) to reduce the injection barriers of hole from anode ITO and attain transport balance of the charge carriers.<sup>18–20</sup> As

<sup>a</sup>Key Laboratory of Functional Materials Physics and Chemistry of the Ministry of Education, Jilin Normal University, Siping 136000, China. E-mail: huaqie@jlnu.edu.cn

<sup>b</sup>College of Information Technology, Jilin Normal University, Siping 136000, China



for as n-type  $C_{60}$  semiconductor, owing to its significant exciton dissociation behavior, it has been used as electron acceptor in photogalvanic cells,<sup>21</sup> while in OLEDs it acts as modifier for electrodes to enhance hole injection.<sup>22–24</sup> Recently organic heterojunction consisting of n-type  $C_{60}$  and p-type pentacene (or CuPc), exhibits excellent charge generation effect and is used as charge generation layers (GGLs) in tandem OLEDs to improved power efficiency.<sup>25,26</sup> Based on the charge generation effect, Chen *et al.*<sup>27</sup> utilized  $C_{60}$ /pentacene heterojunction as HIL to achieve highly efficient OLEDs. This discovery allows the np-type heterojunction to explore novel HIL architecture in OLEDs.

In this work, we reported a yellow PhOLED with high performance through employing np-type  $C_{60}$ /MoO<sub>3</sub> heterojunction as HIL and interfacial exciplex as co-host system. The interfacial exciplex was formed at the interface between 1,3-bis(9H-carbazol-9-yl)benzene (mCP) and (1,3,5-triazine-2,4,6-triyl)tris(benzene-3,1-diyl))tris(diphenylphosphine oxide (PO-T2T). An ultrathin layer of Iridium(III)bis(4-(4-*tert*-butylphenyl)thieno[3,2-*c*]pyridinato-N,C2') acetylacetonate (PO-01-TB) was inserted at the mCP and PO-T2T interface to serve as yellow phosphorescent emitter. The resulting yellow PhOLED exhibited high current efficiency (CE) of 56.7 cd A<sup>-1</sup>, power efficiency (PE) of 71.6 lm W<sup>-1</sup>, and EQE of 17.5%, as well as an extremely low operating voltage of 3.79 V at 1000 cd m<sup>-2</sup>. The achievement of such high performance was mainly attributed to the highly efficient carrier injection based on the np-type hole injector and efficient energy transfer between interfacial exciplex based on the interfacial exciplex co-host and phosphorescent guest.

## 2. Experimental details

All OLEDs were fabricated on clean glass substrates pre-coated indium tin oxide (ITO) with a sheet resistance of 15  $\Omega$  per square. Before evaporation, ITO substrates were cleaned sequentially with acetone, alcohol, and deionized water by scrubbing and sonication, and then dried at 130  $^{\circ}$ C and treated in an ultraviolet-ozone for 15 min before it was loaded into a deposition chamber. All layers were grown on ITO substrate in succession by conventional thermal deposition with the rates of  $\sim 0.1$  nm s<sup>-1</sup> at high vacuum condition ( $\sim 4.0 \times 10^{-4}$  Pa). After the deposition of an Al cathode with a rate of  $>0.1$  nm s<sup>-1</sup>, the devices were completed. All the thicknesses and deposition rates for each layer were monitored *in situ* quartz crystal monitors. The active emission area was determined as 4 mm<sup>2</sup> by the overlap between Al cathode and ITO anode. The photoluminescence (PL) spectra and transient PL decay curves were collected by a Horiba JobinYvon Fluorolog-3 spectrometer with a time-correlated single-photon counting (TCSPC) spectrometer. The current density–voltage–luminance characteristics of all devices were recorded by Keithley 2400 constant current source and SpectraScan PR-655 spectrometer. The CE, PE, and EQE of the OLEDs were calculated from the current density, luminance, and EL spectrum, assuming a Lambertian distribution. All measurements were formed at ambient atmosphere conditions.

## 3. Results and discussion

### 3.1 The formation of exciplex between mCP and PO-T2T

To demonstrate the formation of exciplex between mCP and PO-T2T, we firstly fabricated mCP (20 nm), PO-T2T (20 nm) pure films and mCP:PO-T2T (molar ratio of 1 : 1, 20 nm) doping film, and measured their PL spectra under excitation wavelength of 325 nm as shown in Fig. 1(a). The PL peak of mCP film is located at 375 nm accompanying with shoulder peak at 395 nm. The PO-T2T film exhibits strong emission peak at 384 nm and a weak board emission band at 534 nm. The weak peak is assigned to excimer emission. Compared to the pure mCP and PO-T2T films, a broad emission at 472 nm can be observed in mCP:PO-T2T doping film. Fig. 1(b) depicts the energy level diagram to show the exciplex formation process between mCP and PO-T2T. The emission peak energy 2.63 eV (472 nm) of the mCP:PO-T2T doping film is nearly closed to the energy offset 2.6 eV between the lowest unoccupied molecular orbital (LUMO) level of PO-T2T (3.5 eV) and the highest occupied molecular orbital (HOMO) level of mCP (6.1 eV), suggesting that the broad emission band arises from the mCP:PO-T2T-forming exciplex. In addition, we measured the EL spectra of mCP/PO-T2T and mCP:PO-T2T as shown in Fig. 1(a). The exciplex can also be formed at the mCP/PO-T2T interface. Compared the mCP/PO-T2T double films with mCP:PO-T2T doping film, no obvious change in their EL spectra are observed. In addition, the EL spectrum of the exciplex is almost the same as its PL spectrum.

### 3.2 Exciton distribution in mCP/PO-T2T co-host system

In order to simplify the fabrication process, the double layer structure mCP/PO-T2T was used to replace the doping structure mCP:PO-T2T to fabricated PhOLEDs. Firstly, we fabricated PhOLEDs by introducing yellow phosphor PO-01-TB to elucidate the exciton distribution in mCP/PO-T2T system. The structure of device A1 is illustrated as follows: ITO/mCP(60 nm)/PO-T2T(10 nm)/PO-01-TB(0.1 nm)/PO-T2T(30 nm)/Liq(2 nm)/Al, and the architecture of other devices is ITO/mCP (60–*x* nm)/PO-01-TB(0.1 nm)/mCP(*x* nm)/PO-T2T(40 nm)/Liq(2 nm)/Al, where *x* = 0, 10, 20, and 30 nm corresponding to the device

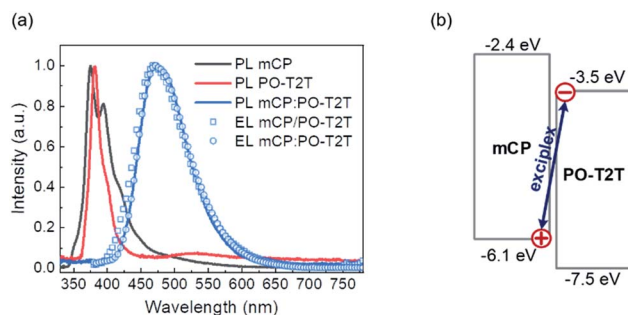


Fig. 1 (a) Photoluminescence (PL) spectra of mCP and PO-T2T pure films, and mCP:PO-T2T doping film on crystal substrates with excitation wavelength of 325 nm. (b) Energy level diagram showing the exciplex formation process between mCP and PO-T2T interface.



A2, A3, A4, and A5, respectively. Here, the emitting layer PO-01-TB is so extremely thin (0.1 nm) that it would insignificantly affect the electrical properties of the resulting device.

Fig. 2(a) shows the normalized EL spectra of the devices A1–A5 at a current density of  $20 \text{ mA cm}^{-2}$ . It can be observed that the emission peak of devices A1–A5 shows significant difference. In detail, as PO-01-TB is employed into PO-T2T layer (device A1), the EL spectrum exhibits two emission peaks. The strong emission at 472 nm should originate from the mCP/PO-T2T-forming interfacial exciplex, while the weak emission at 560 nm can be attributed to PO-01-TB. Fig. 2(b) presents the schematic diagram and the energy levels of the devices A1–A5 with different position of ultrathin PO-01-TB layer. Owing to the large energy barrier for electrons (1.1 eV) and holes (1.4 eV) at the mCP/PO-T2T interface, it is difficult for carriers to cross over the interface. Hence, most holes and electrons should accumulate at the mCP/PO-T2T interface area and generate the interfacial exciplex. Weak emission from PO-01-TB reveals a few exciton can form in the PO-T2T layer. When the PO-01-TB layer is located at the interface of mCP/PO-T2T (device A2), the EL spectrum only shows pure yellow emission at 560 nm with subpeak at 596 nm from PO-01-TB, while the peak of the exciplex is disappear.

Fig. 3 presents the transient PL (TRPL) decay behavior at room temperature for the PO-T2T/mCP and PO-T2T/PO-01-TB/mCP films. Typical two lifetimes of prompt and delayed are observed under 472 nm with mCP/PO-T2T-forming interfacial exciplex. The TRPL signal was fitted by a double-exponential decaying function. The prompt and delayed lifetime of the PO-T2T/mCP film were measured to be longer than that of the PO-T2T/PO-01-TB/mCP film, which is presumably due to the energy transfer process from mCP/PO-T2T-forming interfacial exciplex to PO-01-TB. Considering the  $T_1$  energy level ( $T_1 = 2.69 \text{ eV}$ ) of the mCP/PO-T2T-forming interfacial exciplex<sup>28</sup> higher than that of PO-01-TB ( $T_1 = 2.20 \text{ eV}$ ), and lower than that of mCP (2.90 eV) and PO-T2T (2.99 eV), the efficient energy transfer process can be occurred from the mCP/PO-T2T-forming interfacial exciplex to PO-01-TB emitter, resulting in yellow phosphorescent emission.<sup>29–31</sup> As for as the devices A3–A5, the ultrathin PO-01-TB layer is inserted into mCP layer (*i.e.*  $x = 10, 20, 30$ ) away from the interface of mCP/PO-T2T, two emission

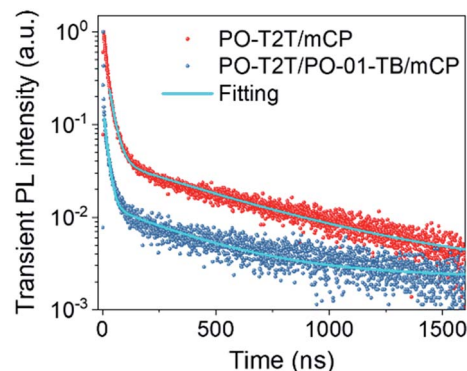


Fig. 3 The transient PL decayed curves of the PO-T2T/mCP and PO-T2T/PO-01-TB/mCP films at 300 K.

peaks from the exciplex (472 nm) and PO-01-TB (560 nm) appears simultaneously. Because of its shallower HOMO levels than that of mCP, PO-01-TB can act as a hole trap for carriers when doped in mCP and recombine at the PO-01-TB layer. With increasing the values of  $x$ , the decreasing hole carrier concentration results in the decrease in the relative emission intensity from PO-01-TB.

### 3.3 PhOLED based on np-type $\text{C}_{60}/\text{MoO}_3$ composited HIL

According to the discussion above, inserting the ultrathin PO-01-TB layer in mCP/PO-T2T interface can benefit to realize pure yellow emission through complete energy transfer. In order to achieve high efficiency of PO-01-TB based PhOLEDs, we proposed to employ np-type  $\text{C}_{60}/\text{MoO}_3$  heterojunction as HIL and interfacial exciplex as host. The device configuration is as follows: ITO/HIL/mCP(60 nm)/PO-01-TB(0.1 nm)/PO-T2T (40 nm)/LiQ(2 nm)/Al. For a conventional device HIL is  $\text{MoO}_3$ (5 nm) (device B1). For np-type devices, HIL is  $\text{C}_{60}$ (1 nm)/ $\text{MoO}_3$ ( $y$  nm), where  $y = 4, 3, 2$ , and 1 nm corresponding to devices B2, B3, B4, and B5, respectively. Fig. 4 shows the energy diagram and the normalized EL spectra of the devices B1–B5. The five devices exhibit almost same EL spectra with the emission peak at 560 nm from PO-01-TB, indicating that the change in HIL structure could not affect the emission property of the devices.

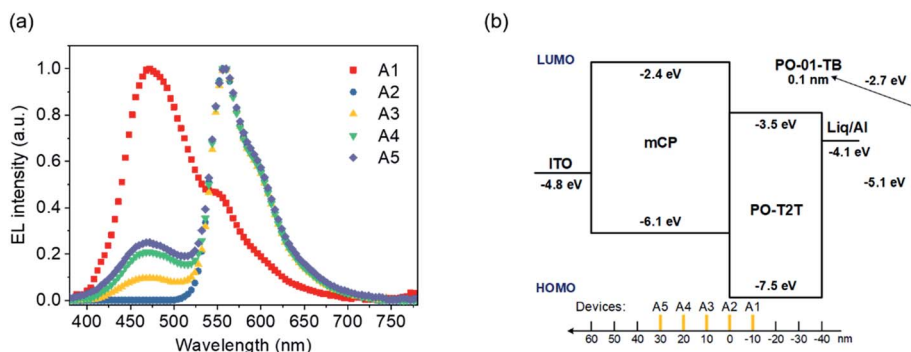


Fig. 2 (a) EL spectra of the devices A1–A5 at  $20 \text{ mA cm}^{-2}$ . (b) The structures of the devices A1–A5 and the detailed energy level diagram of the materials. The bottom gives the distance of PO-01-TB to the interface of mCP/PO-T2T in devices A1–A5.



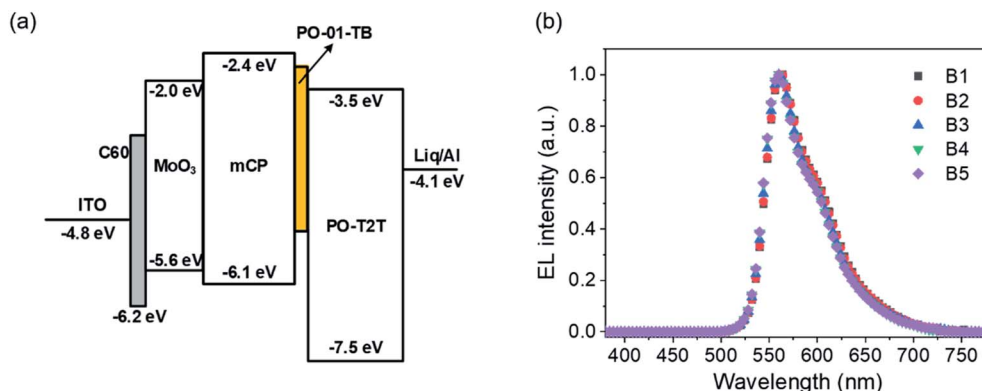


Fig. 4 (a) Structure and the energy diagram and (b) EL spectra of the devices B1–B5.

From Fig. 5(a), the current density of the devices B2–B5 fabricated utilizing a np-type C60/MoO<sub>3</sub> HIL is higher than that of the device B1 fabricated with a MoO<sub>3</sub> HIL at the same operating voltage. This could be attributed to enhancement of hole injection ability of np-type C60/MoO<sub>3</sub> HIL. The main EL performances of all devices are summarized in Table 1. The

turn-on voltage (at 1 cd m<sup>-2</sup>) of the device B1 and the devices B2–B5 are 2.70 V and about 2.46–2.55 V. The rather low turn-on voltage of 2.46 V for device B3 is very close to the thermodynamic limit, indicating that almost no potential barrier for hole injection is presented due to the introduction of C<sub>60</sub> layer. In addition, the voltage of the devices B2–B5 decrease significantly

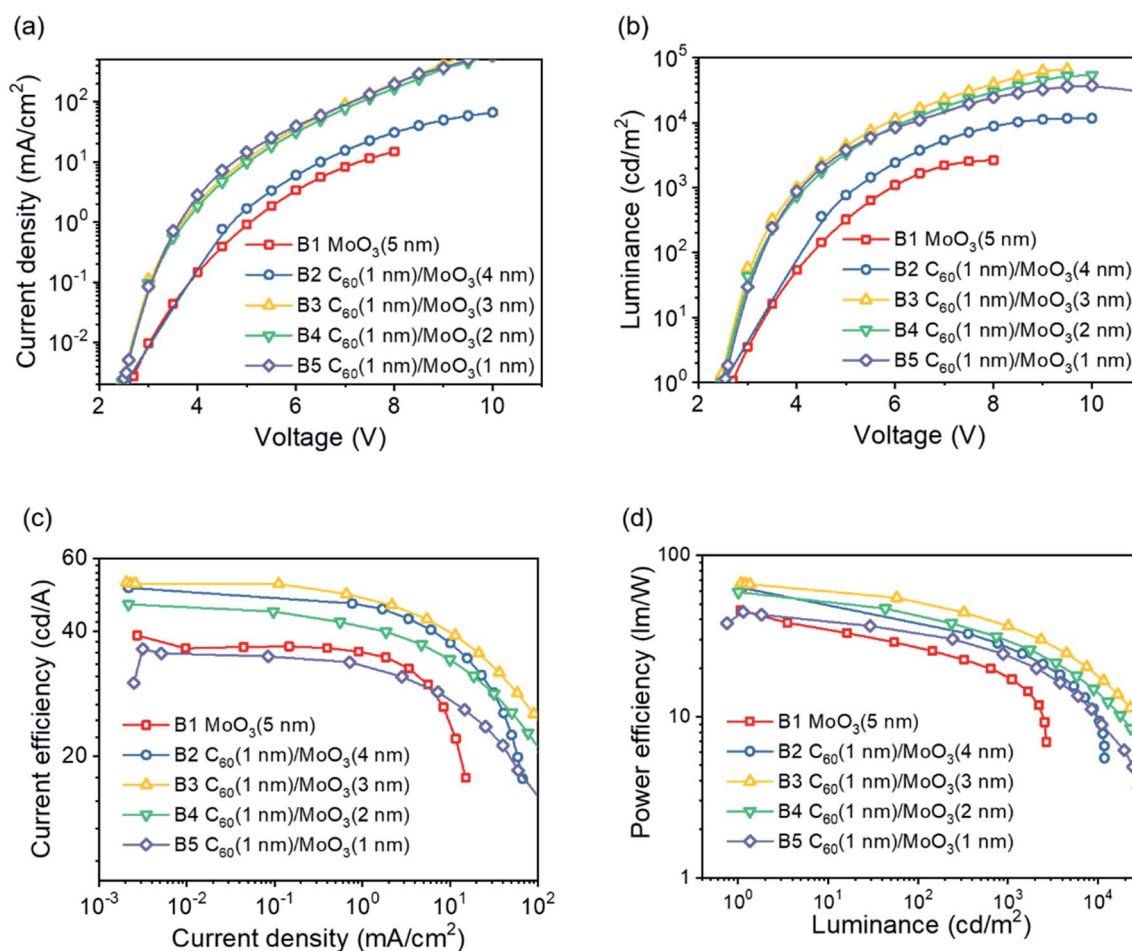


Fig. 5 Comparison of the EL performances of devices B1–B5: (a) Current density–voltage ( $J$ – $V$ ) characteristics; (b) Luminance–voltage ( $L$ – $V$ ) characteristics; (c) Current efficiency–current density (CE– $J$ ) characteristics; (d) Power efficiency–luminance (PE– $L$ ) characteristics.



Table 1 Summary of EL performances of devices B1–B5 and C1–C3

Device	Voltage (V)	Maximum	@1000 cd m <sup>-2</sup>	@5000 cd m <sup>-2</sup>
	@1 <sup>a</sup> /1000/5000 cd m <sup>-2</sup>	EQE <sup>b</sup> /CE <sup>c</sup> /PE <sup>d</sup> (%/cd A <sup>-1</sup> /lm W <sup>-1</sup> )		
B1	2.70/5.92/—	12.5/39.1/45.5	10.0/32.8/17.4	—
B2	2.55/5.24/6.85	16.4/51.0/62.9	13.4/44.0/26.9	10.6/35.3/16.1
B3	2.46/3.99/5.06	16.5/52.6/67.2	13.7/46.4/36.4	11.4/38.8/24.1
B4	2.47/4.13/5.33	14.4/47.5/59.2	11.6/39.3/30.0	9.5/32.2/19.1
B5	2.53/4.05/5.28	11.5/36.3/44.7	9.0/34.1/24.0	7.2/24.6/14.7
C1	2.48/4.24/5.41	14.2/47.9/55.2	12.7/43.1/31.4	10.5/34.9/20.7
C2	2.43/3.86/4.76	17.5/56.8/71.6	15.1/52.1/41.5	12.7/43.6/29.1
C3	2.51/4.59/5.92	16.0/51.1/62.4	14.3/48.3/32.1	11.7/38.4/20.9

<sup>a</sup> Turn-on voltage at a brightness of 1 cd m<sup>-2</sup>. <sup>b</sup> External quantum efficiency. <sup>c</sup> Current efficiency. <sup>d</sup> Power efficiency.

compared with the device B1 at the same luminance as shown in Fig. 5(b). The operating voltages (at 1000 cd m<sup>-2</sup>) of devices B1, B2, B3, B4, and B5 are 5.92, 5.24, 3.99, 4.13, and 4.05 V, respectively. The operating voltage of the device B3 is reduced by 32.6% compared to that of device B1. Therefore, compared with the device B1, the current density and luminance of device B2–B5 with C<sub>60</sub>/MoO<sub>3</sub> as HIL are obviously improved.

Considering the low hole mobility ( $2.8 \times 10^{-7}$  cm<sup>2</sup> Vs<sup>-1</sup>)<sup>32</sup> and high HOMO energy level (6.2 eV),<sup>33</sup> the C<sub>60</sub> layer may block parts of the holes injection from the anode ITO to MoO<sub>3</sub> in the devices B2–B5, and one can predict that the current density should decrease and the turn-on voltage increases. However, in our work, the C<sub>60</sub>-containing devices B2–B5 show lower turn-on voltage and higher current density than the device B1. This means that the hole injection efficiency is significantly enhanced due to the introduction of np-type C<sub>60</sub>/MoO<sub>3</sub> HIL, which is consistent with the reported results for C<sub>60</sub>/pentacene as the hole injector in ref. 27. According to the “p–n junction” characteristic of C<sub>60</sub>/MoO<sub>3</sub> heterojunction, free carriers can be effectively generated at the C<sub>60</sub>/MoO<sub>3</sub> interface. Then, under the applied electrical field, the generated electrons can be extracted from LUMO of C<sub>60</sub> to the ITO, while the generated holes are easily injected from HOMO of MoO<sub>3</sub> into mCP, and combine with the electrons injected from the cathode to form the exciplex at mCP/PO-T2T interface. Subsequently the exciplex transfer its energy to PO-01-TB and then achieving yellow phosphorescent emission. From Fig. 5(c), (d) and Table 1, the device B3 exhibits a high CE, PE, and EQE of 52.6 cd A<sup>-1</sup>, 67.2 lm W<sup>-1</sup>, 16.5%, respectively, which are increased by approximately 34.5%, 47.7%, and 32% compared to that of the device B1 (only MoO<sub>3</sub> as HIL). It is vital to point out that the efficiency–luminance roll-off of the device B3 is relatively mild with respect to the device B1. With the luminance rising to 1000 cd m<sup>-2</sup> (2.16 mA cm<sup>-2</sup>), the CE, PE, and EQE could be kept at 46.4 cd A<sup>-1</sup>, 36.4 lm W<sup>-1</sup>, and 13.7%, respectively. Thus, the further enhanced EL performances of the device B3 should be ascribed to the increasing electric field on C<sub>60</sub>/MoO<sub>3</sub> heterojunction due to the decreasing thickness of MoO<sub>3</sub> film.

In order to deeply understand the hole transporting properties of np-type C<sub>60</sub>/MoO<sub>3</sub> HIL, the hole-only single-carrier devices with structure of ITO/C<sub>60</sub>(1 nm), MoO<sub>3</sub>(5 nm), or C<sub>60</sub>(1

nm)/MoO<sub>3</sub>(3 nm)/mCP(60 nm)/PO-01-TB(0.1 nm)/PO-T2T(10 nm)/mCP(30 nm)/Al were fabricated. The *J*–*V* characteristics of these devices are displayed in Fig. 6. A comparison of the current density at the same operating voltage of the hole-only devices clearly indicates that the hole current in the np-type C<sub>60</sub>/MoO<sub>3</sub> HIL device is higher than that in the C<sub>60</sub> and MoO<sub>3</sub> HIL devices, which can be attributed to the improved conductivity of the HIL with the np-type C<sub>60</sub>/MoO<sub>3</sub>. The results clearly demonstrate that the np-type C<sub>60</sub>/MoO<sub>3</sub> heterojunction does be an effective hole injector to realize high performance OLEDs.

One key design of device B3 is the introduction of C<sub>60</sub>/MoO<sub>3</sub> composite as HIL. To optimize the EL properties of device B3, the comparable devices were fabricated with structure of ITO/C<sub>60</sub> (*x* nm)/MoO<sub>3</sub>(3 nm)/mCP(60 nm)/PO-01-TB(0.1 nm)/PO-T2T(40 nm)/LiQ(2 nm)/Al, while *x* = 0.5, 2, 3 nm corresponds to devices C1–C3, respectively. Except of the thickness of C<sub>60</sub> layer, other layers are kept the same as the device B3. Fig. 7 shows the *J*–*V*, *L*–*V*, CE–*J*, and PE–*L* characteristics of devices C1–C3 and B3, and the key performance parameters are summarized in Table 1. The resulting OLEDs performance in operating voltage and efficiency exhibits the dependence on the thickness of C<sub>60</sub> layer. The current density first increases with the thickness *x* of C<sub>60</sub> from 0.5 to 2 nm, and then it decreases as further increasing *x* to 3 nm. Moreover, at the luminance of

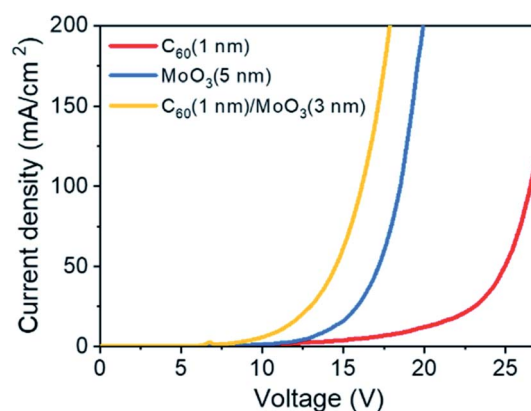


Fig. 6 Current density–voltage (*J*–*V*) characteristics of hole-only devices.



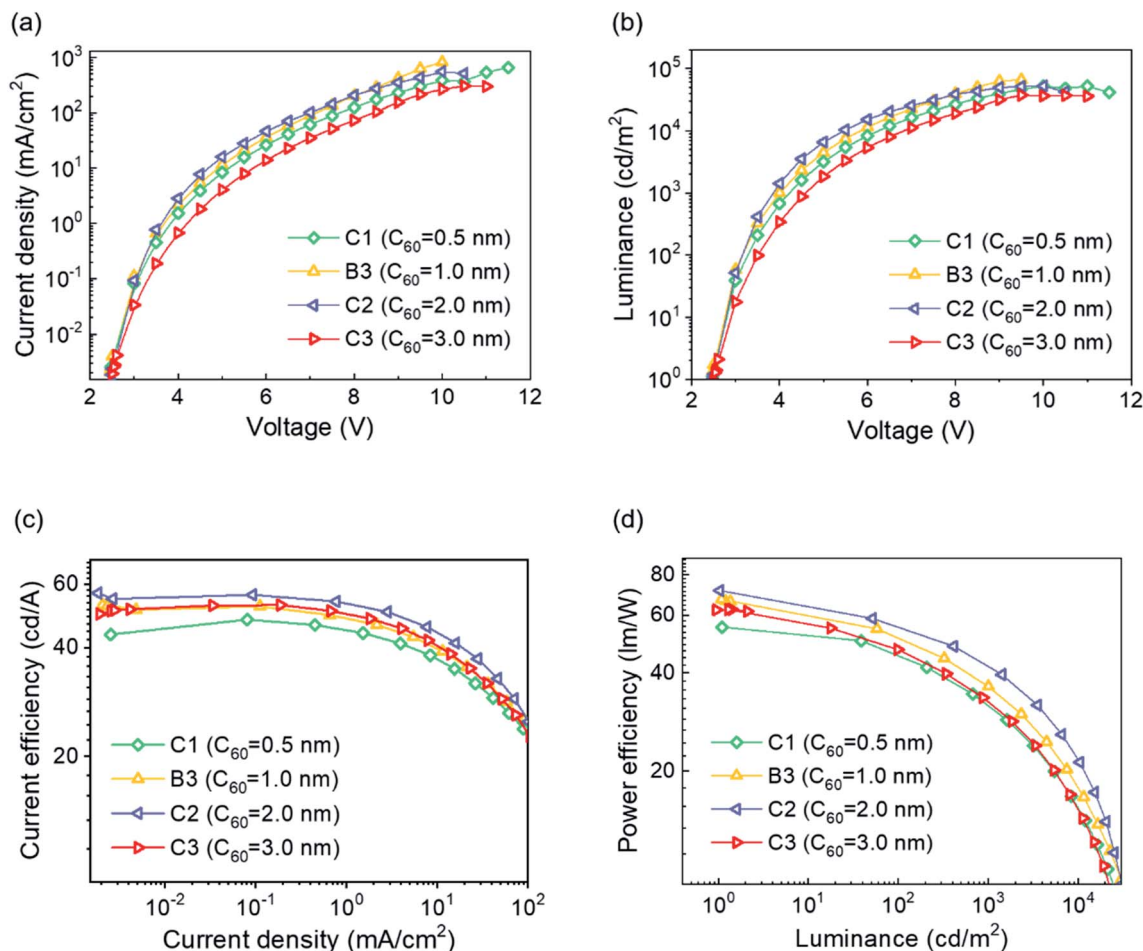


Fig. 7 EL performances of devices C1–C3 and B3 with the different thickness of  $C_{60}$  layer. (a) Current density–voltage ( $J$ – $V$ ) characteristics. (b) Luminance–voltage ( $L$ – $V$ ) characteristics. (c) Current efficiency–luminance (CE– $L$ ) characteristics. (d) Power efficiency–luminance (PE– $L$ ) characteristics.

1000  $\text{cd m}^{-2}$ , the operating voltages are 4.24, 3.99, 3.86, and 4.59 V for the devices with  $x = 0.5, 1, 2$ , and 3 nm, respectively (shown in Fig. 7(b)). These results indicate that properly increasing the thickness of  $C_{60}$  is beneficial to the formation of excellent np-junction  $C_{60}/\text{MoO}_3$  for the efficient charge generation and injection. However, the low hole mobility and high HOMO energy level of  $C_{60}$  will inferior for hole injection and transport,<sup>23</sup> which results in low current density and high operating voltage in device C3 with 3 nm- $C_{60}$  layer. The device C2 ( $x = 2$  nm) shows the best performance with a maximum CE, PE, and EQE of 56.8  $\text{cd A}^{-1}$ , 71.6  $\text{lm W}^{-1}$ , and 17.5%, respectively. Notably, the CE still keep as high as 52.1% at 1000  $\text{cd m}^{-2}$  (1.97  $\text{mA cm}^{-2}$ ), showing extremely low efficiency roll-off of 8.3%.

## 4. Conclusion

We have achieved a high performance yellow PhOLEDs with doping-free structure by using ultrathin PO-01-TB layer inserted in mCP/PO-T2T interface as emitter and np-type  $C_{60}/\text{MoO}_3$  composite film as HIL. More free charge carriers could be

supplied in np-type  $C_{60}/\text{MoO}_3$  heterojunctions. The yellow emission was originated from the completely energy transfer from mCP/PO-T2T-forming interfacial exciplex to PO-01-TB. By optimizing the thickness of  $C_{60}$ , high-performance PhOLED with  $C_{60}$  (2 nm)/ $\text{MoO}_3$  (3 nm) as HIL was achieved with maximum CE of 56.7  $\text{cd A}^{-1}$ , PE of 71.6  $\text{lm W}^{-1}$ , and EQE of 17.5%, as well as low operating voltage of 3.79 V (at 1000  $\text{cd m}^{-2}$ ) and a lower CE efficiency roll-off of 8.3%. The work provides a simple structure design for fabricating highly efficient PhOLEDs with low operating voltage simultaneously. Moreover, doping-free structure can satisfy the requirement on the large-scale industrialized requirement.

## Conflicts of interest

There are no conflicts of interest to declare.

## Acknowledgements

This work was supported by National Natural Science Foundation of China under Contract No. 11774134.



## References

- 1 S. R. Forrest, The path to ubiquitous and low-cost organic electronic appliances on plastic, *Nature*, 2004, **428**, 911–918.
- 2 S. Reineke, F. Lindner, G. Schwartz, N. Seidler, K. Walzer, B. Lüssem and K. Leo, White organic light-emitting diodes with fluorescent tube efficiency, *Nature*, 2009, **459**, 234–238.
- 3 J. Zeng, J. Guo, H. Liu, Z. Zhao and B. Tang, A Multifunctional Bipolar Luminogen with Delayed Fluorescence for High-Performance Monochromatic and Color-Stable Warm-White OLEDs, *Adv. Funct. Mater.*, 2020, **30**, 2000019.
- 4 S. Reineke, M. Thomschke, B. Lüssem and K. Leo, White organic light-emitting diodes: status and perspective, *Rev. Mod. Phys.*, 2013, **85**, 1245–1291.
- 5 M. A. Baldo, D. O'Brien, Y. You, A. Shoustikov, S. Sibley, M. Thompson and S. R. Forrest, Highly efficient phosphorescent emission from organic electroluminescent devices, *Nature*, 1998, **395**, 151–154.
- 6 K. Udagawa, H. Sasabe, C. Cai and J. Kido, Low-driving-voltage blue phosphorescent organic light-emitting devices with external quantum efficiency of 30%, *Adv. Mater.*, 2014, **26**, 5062–5066.
- 7 D. Zhang, M. Cai, Y. Zhang, D. Zhang and L. Duan, Highly efficient simplified single emitting-layer hybrid WOLEDs with low roll-off and good color stability through enhanced Förster energy transfer, *ACS Appl. Mater. Interfaces*, 2015, **7**, 28693–28700.
- 8 L. Zhu, Z. Wu, J. Chen and D. Ma, Reduced efficiency roll-off in all-phosphorescent white organic light-emitting diodes with an external quantum efficiency of over 20%, *J. Mater. Chem. C*, 2015, **3**, 3304–3310.
- 9 S. Zhang, J. Yao, Y. Dai, Q. Sun, D. Yang, X. Qiao, J. Chen and D. Ma, High efficiency and color quality undoped phosphorescent white organic light-emitting diodes based on simple ultrathin structure in exciplex, *ACS Appl. Mater. Interfaces*, 2020, **85**, 105821.
- 10 H. V. Eersel, P. A. Bobbert, R. A. J. Janssen and R. Coehoorn, Monte Carlo study of efficiency roll-off of phosphorescent organic light-emitting diodes: Evidence for dominant role of triplet-polaron quenching, *Appl. Phys. Lett.*, 2014, **105**(14), 143303.
- 11 D. Zhang, M. Cai, Y. Zhang, D. Zhang and L. Duan, Highly Efficient Simplified Single-Emitting-Layer Hybrid WOLEDs with Low Roll-off and Good Color Stability through Enhanced Förster Energy Transfer, *ACS Appl. Mater. Interfaces*, 2015, **7**, 28693–28700.
- 12 W. Song, H. L. Lee and J. Y. Lee, High triplet energy exciplex hosts for deep blue phosphorescent organic light-emitting diodes, *J. Mater. Chem. C*, 2017, **5**, 5923–5929.
- 13 R. Sheng, A. Li, F. Zhang, J. Song, Y. Duan and P. Chen, Highly efficient, simplified monochrome and white organic light-emitting devices based on novel exciplex host, *Adv. Opt. Mater.*, 2019, **8**(2), 1901247.
- 14 Y. Zhao, J. Zhang, Y. Miao, X. Wei, H. Xu, Y. Wu, H. Wang, T. Li and B. Xu, All-fluorescent white organic light-emitting diodes with EQE exceeding theoretical limit of 5% by incorporating a novel yellow fluorophor in co-doping forming blue exciplex, *ACS Appl. Mater. Interfaces*, 2020, **83**, 105746.
- 15 Q. Tian, L. Zhang, Y. Hu, S. Yuan, Q. Wang and L. Liao, High-Performance White Organic Light-Emitting Diodes with Simplified Structure Incorporating Novel Exciplex-Forming Host, *ACS Appl. Mater. Interfaces*, 2018, **10**(45), 39116–39123.
- 16 Y. Park, S. Lee, K. Kim, S. Kim, J. Lee and J. Kim, Exciplex-forming co-host for organic light-emitting diodes with ultimate efficiency, *Adv. Funct. Mater.*, 2013, **23**, 4914–4920.
- 17 J. Wang, X. Zhang, L. Fan, X. Zhang and W. Huang, Highly efficient solution-processed red phosphorescent organic light-emitting diodes employing an interface exciplex host, *J. Mater. Chem. C*, 2020, **8**, 9909–9915.
- 18 I. H. Hong, M. W. Lee, Y. M. Koo, H. Jeong, T. S. Kim and O. K. Song, Effective hole injection of organic light-emitting diodes by introducing buckminsterfullerene on the indium tin oxide anode, *Appl. Phys. Lett.*, 2005, **87**(6), 063502.
- 19 M. Kröger, S. Hamwi, J. Meyer, T. Riedl, W. Kowalsky and A. Kahn, Role of the deep-lying electronic states of MoO<sub>3</sub> in the enhancement of hole-injection in organic thin films, *Appl. Phys. Lett.*, 2009, **95**(12), 123301.
- 20 H. Xu and Z. Xiang, Investigation of hole injection enhancement by MoO<sub>3</sub> buffer layer in organic light emitting diodes, *J. Appl. Phys.*, 2013, **114**(24), 026105.
- 21 J. Y. Lee, Efficient hole injection in organic light-emitting diodes using C<sub>60</sub> as a buffer layer for Al reflective anodes, *Appl. Phys. Lett.*, 2006, **88**(7), 3–6.
- 22 Z. Lv, Z. Deng, D. Xu, X. Li and Y. Jia, Efficient organic light-emitting diodes with C<sub>60</sub> buffer layer, *Displays*, 2009, **30**(1), 23–26.
- 23 S. H. Kim, J. Jang and J. Y. Lee, Relationship between indium tin oxide surface treatment and hole injection in C<sub>60</sub> modified devices, *Appl. Phys. Lett.*, 2006, **89**(25), 60–62.
- 24 D. D. Song, S. L. Zhao, F. J. Zhang, Z. Xu, J. M. Li, X. Yue, H. N. Zhu, L. F. Lu and Y. S. Wang, A key issue of organic light-emitting diodes: Enhancing hole injection by interface modifying, *J. Lumin.*, 2009, **129**(12), 1978–1980.
- 25 Y. Chen, J. Chen, D. Ma, D. Yan and L. Wang, Tandem white phosphorescent organic light-emitting diodes based on interface-modified C<sub>60</sub>/pentacene organic heterojunction as charge generation layer, *Appl. Phys. Lett.*, 2011, **99**, 103304.
- 26 D. Zhao, H. Liu, Y. Miao, H. Wang, B. Zhao, Y. Hao, F. Zhu and B. Xu, A red tandem organic light-emitting diode based on organic photovoltaic-type charge generation layer, *Org. Electron*, 2016, **32**, 1–6.
- 27 Y. Chen, D. Ma, H. Sun, J. Chen, Q. Guo, Q. Wang and Y. Zhao, Organic semiconductor heterojunctions: electrode-independent charge injectors for high-performance organic light-emitting diodes, *Light: Sci. Appl.*, 2016, **5**, 16042.
- 28 C. Zheng, D. Chen, X. Zhang, C. Lee, W. Liu, J. Chen, F. Li, Y. Dong, X. Ou and K. Wang, Novel strategy to develop exciplex emitters for high-performance OLEDs by



- employing thermally activated delayed fluorescence materials, *Adv. Funct. Mater.*, 2016, **26**(12), 2002–2008.
- 29 B. Zhao, T. Zhang, B. Chu, W. Li, Z. Su, Y. Luo, R. Li, X. Yan, F. Jin and Y. Gao, Highly efficient tandem full exciplex orange and warm white OLEDs based on thermally activated delayed fluorescence mechanism, *ACS Appl. Mater. Interfaces*, 2015, **17**, 15–21.
- 30 T. Xu, M. Yang, M. J. Liu, X. Wu, I. Murtaza, G. He and H. Meng, Wide color-range tunable and low roll-off fluorescent organic light emitting devices based on double undoped Ultrathin emitters, *Org. Electron*, 2016, **37**, 93–99.
- 31 Q. Wu, S. Zhang, S. Yue, Z. Zhang, G. Xie, Y. Zhao and S. Liu, Enhanced efficiency in single-host white organic light-emitting diode by triplet exciton conversion, *J. Lumin.*, 2013, **143**, 108–112.
- 32 R. Pandey, A. A. Gunawan, K. A. Mkhoyan and R. J. Holmes, Efficient Organic Photovoltaic Cells Based on Nanocrystalline Mixtures of Boron Subphthalocyanine Chloride and C<sub>60</sub>, *Adv. Funct. Mater.*, 2012, **22**, 617–624.
- 33 S. Yoo, B. Domercq and B. Kippelen, Efficient thin-film organic solar cells based on pentacene/C<sub>60</sub> heterojunctions, *Appl. Phys. Lett.*, 2004, **85**, 5427–5429.

